PARP-1 and PARP-2 interact with nucleophosmin/B23 and accumulate in transcriptionally active nucleoli

Véronique S. Meder[1], Marcel Boeglin[2], Gilbert de Murcia[1] and Valérie Schreiber[1,*]

[1]UPR 9003 du Centre National de la Recherche Scientifique. Laboratoire conventionné avec le Commissariat à l'Energie Atomique, Université Louis Pasteur, Ecole Supérieure de Biotechnologie de Strasbourg, Boulevard Sébastien Brant, BP10413, 67412 Illkirch, France
[2]Institut de Génétique et de Biologie Moléculaire et Cellulaire, CNRS/INSERM/ULP, Collège de France, BP 163, 67404 Illkirch, France
*Author for correspondence (e-mail: schreibe@esbs.u-strasbg.fr)

Accepted 25 October 2004
Journal of Cell Science 118, 211-222 Published by The Company of Biologists 2005
doi:10.1242/jcs.01606

Summary

The DNA damage-dependent poly(ADP-ribose) polymerases-1 and -2 (PARP-1 and PARP-2) are survival factors that share overlapping functions in the detection, signaling and repair of DNA strand breaks resulting from genotoxic lesions in mammalian cells. Here we show that PARP-1 and PARP-2 subnuclear distributions partially overlap, with both proteins accumulating within the nucleolus independently of each other. PARP-2 is enriched within the whole nucleolus and partially colocalizes with the nucleolar factor nucleophosmin/B23. We have identified a nuclear localization signal and a nucleolar localization signal within the N-terminal domain of PARP-2. PARP-2, like PARP-1, interacts with B23 through its N-terminal DNA binding domain. This association is constitutive and does not depend on either PARP activity or ribosomal transcription, but is prevented by mutation of the nucleolar localization signal of PARP-2. PARP-1 and PARP-2, together with B23, are delocalized from the nucleolus upon RNA polymerase I inhibition whereas the nucleolar accumulation of all three proteins is only moderately affected upon oxidative or alkylated DNA damage. Finally, we show that murine fibroblasts deficient in PARP-1 or PARP-2 are not affected in the transcription of ribosomal RNAs. Taken together, these results suggest that the biological role of PARP-1 and PARP-2 within the nucleolus relies on functional nucleolar transcription, without any obvious implication of either PARP on this major nucleolar process.

Key words: Cellular response to DNA damage, Poly(ADP-ribosyl)ation, PARP homologues, Nuclear and nucleolar localization signals

Introduction

Among the cellular responses to DNA strand breaks, local poly(ADP-ribose) synthesis is immediate and triggers the recruitment of repair factors at the damaged site, thus conditioning the efficiency of the repair process. Poly(ADP-ribose) polymerases-1 and -2 (PARP-1 and PARP-2) are the only known enzymes mediating DNA-dependent poly(ADP-ribose) synthesis in response to DNA damage. They both belong to a superfamily of 18 PARPs that include the centrosomal PARP-3, the vault-particle associated PARP-4 and the telomeric and Golgi tankyrases-1 and -2 (Amé et al., 2004). Poly(ADP-ribose) is a branched polyanion produced by the polymerization of ADP-ribose moieties from NAD^+ and is covalently but transiently bound to acceptor proteins. Proteins poly(ADP-ribosyl)ated by PARP-1 and PARP-2 are mainly involved in chromatin structure and DNA metabolism. Histones H1 and H2B, when integrated into nucleosomes, can be poly(ADP-ribosyl)ated by PARP-1 and PARP-2 respectively (Schreiber et al., 2005). This epigenetic modification that occurs in the presence of DNA strand breaks leads to the loosening and opening of the chromatin structure likely to favor the access of proteins involved in repair, replication, recombination or transcription (for a review, see Rouleau et al., 2004).

Inactivation of *PARP-1* or *PARP-2* genes in the mouse revealed the involvement of both proteins in the surveillance and maintenance of genome integrity. Both deficient mouse strains were sensitive to ionizing radiation. Upon treatment with alkylating agents, cells derived from these mice displayed an elevated number of chromosomes and chromatid breaks, a prolonged G2/M cell cycle arrest and a delay in the rejoining of DNA damage-induced strand breaks (Ménissier de Murcia et al., 1997; Menissier de Murcia et al., 2003; Schreiber et al., 2002). Both PARPs share several common partners in base excision repair and single strand break repair (BER/SSBR) such as XRCC1, DNA pol β and DNA ligase III (Schreiber et al., 2002). Despite the fact that PARP-1 and PARP-2 can heterodimerize and heteromodify each other in vitro, it was not clear whether they intervene together or separately at a distinct step of the repair process. Recent findings demonstrate that PARP-1, through local polymer synthesis, efficiently attracts XRCC1 at the site of the DNA break (Okano et al., 2003), whereas PARP-2 is likely to participate in a later step (Amé et al., 2004).

Accumulation of PARP-1 in the nucleolus of interphase cells has been documented (Desnoyers et al., 1996; Fakan et al., 1988; Mosgoeller et al., 1996). Proteomic analyses of the nucleolus also revealed the presence of PARP-1 (Andersen et al., 2002; Scherl et al., 2002). In addition, co-purification of the nucleolar proteins B23 (nucleophosmin) or C23 (nucleolin)

and PARP-1 (Borggrefe et al., 1998), as well as their poly(ADP-ribosyl)ation following γ irradiation was reported (Leitinger and Wesierska-Gadek, 1993; Ramsamooj et al., 1995), but the function of PARP-1 in the nucleolus is still under investigation.

The primary established function of the nucleolus is ribosome biosynthesis through transcription by RNA polymerase (pol) I of a 47S RNA precursor (pre-rRNA) that is processed to give the 18S, 5.8S and 28S rRNAs, which are then assembled with ribosomal proteins into pre-ribosomal particles. The human rDNA genes are tandemly repeated in approximately 180 copies on chromosomes 13, 14, 15, 21 and 22, but only half of the repeats are transcriptionally active in a cycling cell. The nucleolus is morphologically separated into three distinct areas, reflecting the vectorial process of ribosome biogenesis (Dundr and Misteli, 2001). Transcription of rRNAs takes place at the border of the fibrillar centers (FC) and the dense fibrillar components (DFC). Then, maturation of the rRNAs and assembly of the pre-ribosomal particles occurs in the surrounding granular components (GC).

The plurifunctionality of the nucleolus was revealed through many reports describing its involvement in several processes such as maturation or export of some mRNAs, tRNAs and ribonucleoproteins, proliferation control, mitotic regulation and control of aging (reviewed by Dundr and Misteli, 2001). One of the more intriguing novel roles of the nucleolus is the sensing of cellular stress and transmission of signals leading to the regulation of p53 abundance and activity (Rubbi and Milner, 2003).

In order to evaluate whether PARP-2, like PARP-1, is a nucleolar protein, we examined its subcellular distribution in murine and human cells. We demonstrated that PARP-2 accumulates within the nucleolus of mammalian cells independently of PARP-1. We identified a nuclear localization signal (NLS) and a nucleolar localization signal (NoLS) both present within the DNA binding domain. The NoLS, localized at the extreme N-terminus of PARP-2 is sensitive to structural constraints. The nucleolar factor B23 interacts with both PARP-1 and PARP-2 and this association is not altered upon DNA damage, PARP inhibition or RNA pol I inhibition. PARP-1 and PARP-2 are delocalized from the nucleolus when cells are treated with RNA pol I inhibitors, but not with RNA pol II inhibitors. Genotoxic agents generating alkylated or oxidative DNA lesions only moderately affect the nucleolar accumulation of PARPs. Finally, PARP-1 and PARP-2 deficient cells are not altered in their nucleolar ribosomal transcription efficiency. Thus, although efficient nucleolar transcription is required for nucleolar accumulation of PARP-1 and PARP-2, both PARPs are dispensable for ribosomal RNA transcription.

Materials and Methods

Plasmids

Plasmids encoding GFP-mPARP-2 and GFP-mPARP-$2_{1\text{-}69}$ are described (Schreiber et al., 2002; Amé et al., 1999). GFP-NLS-SV was obtained by inserting complementary oligonucleotides encoding the SV40 large-T (SV40-T) antigen NLS (Schreiber et al., 1992) into the *Kpn*I site of pEGFP-C3 (Clontech). A *Nru*I/*Bst*YI fragment from pBCmPARP-2 (Schreiber et al., 2002) was subcloned into *Sca*I/*Bam*HI sites of pEGFP-C3 allowing the expression of GFP-mPARP-$2_{1\text{-}211}$. GFP-mPARP-$2_{15\text{-}50}$ was obtained by cloning into the *Eco*RI site of pEGFP-C3, a PCR fragment encoding residues 15-50 of mPARP-2. The GFP-mPARP$2_{33\text{-}46}$ expressing plasmid was generated by inserting complementary oligonucleotides encoding residues 33-46 of mPARP-2 into the *Eco*RI/*Bam*HI sites of pEGFP-C3. GFP-NLS-mPARP-$2_{63\text{-}202}$ was obtained by ligating a *Bam*HI/*Bam*HI fragment taken from the plasmid encoding GST-mPARP-$2_{63\text{-}202}$ (Schreiber et al., 2002) into the *Bam*HI site of the plasmid encoding GFP-NLS-SV. GFP-NLS-mPARP-$2_{202\text{-}559}$ was obtained by cloning a PCR fragment encoding residues 202-559 of mPARP-2 into the *Sma*I site of the plasmid encoding GFP-NLS-SV. A *Bam*HI/*Bam*HI fragment encoding human PARP-2 (hPARP-2, from Altana Pharma, Konstanz, Germany) was subcloned into the *Bam*HI site of pEGFP-C1, allowing the expression of GFP-hPARP-2. A *Sma*I/*Pst*I fragment from pVLmPARP-2 (Amé et al., 1999) was subcloned into the *Eco*47III/*Pst*I sites of pEGFP-N1. The *Pst*I/*Sma*I fragment was then replaced by a *Pst*I/*Eco*RV linker encoding the last three residues of murine PARP-2 but no stop codon, allowing the expression of mPARP-2-GFP. The *Pml*I/*Eco*RV fragment was replaced by a *Pml*I/*Sma*I fragment of pEGFP-mPARP-$2_{1\text{-}69}$, allowing the expression of mPARP-$2_{1\text{-}69}$-GFP. A *Bam*HI/*Stu*I fragment encoding residues 1-71 of hPARP-2 was subcloned into the *Bgl*II/*Sma*I sites of pEGFP-C1 or pEGFP-N1, allowing the expression of GFP-hPARP-$2_{1\text{-}71}$ or hPARP-$2_{1\text{-}71}$-GFP, respectively. PCR was performed on the plasmid encoding mPARP-$2_{1\text{-}69}$-GFP, with the 5′ oligonucleotide: 5′-GAGCGCT-AGCGGGGGGGAGGATGGCGCCGGCCGCAGCTGCATCAGGC-TTGGAAGGAGTGC-3′ and a 3′ oligonucleotide hybridizing to the N-terminal part of GFP. The PCR product was subcloned into the *Nhe*I/*Sma*I sites of pEGFP-N1, allowing the expression of mPARP-$2_{1\text{-}69}A_{4\text{-}7}$-GFP. Plasmids encoding GST-fusion proteins are described (Schreiber et al., 2002). GST-hPARP-2 was obtained by inserting a *Bam*HI/*Not*I fragment encoding hPARP-2 into the *Bam*HI/*Not*I sites of pBC2. pBC2 was created by religating a *Nru*I/*Eco*RI digested and filled-in pBC vector (Chatton et al., 1995).

Cell culture and DNA transfections

Wild type (WT), PARP-$1^{-/-}$ and PARP-$2^{-/-}$ primary mouse embryonic fibroblasts were used between the first and fourth passage (Menissier de Murcia et al., 2003). For transfection experiments, cells grown on glass coverslips were transfected by the calcium phosphate coprecipitation method with 2 μg plasmid DNA. The medium was replaced 24 hours later and observation of living cells was performed 48 hours post-transfection by epifluorescence with a Leica DMRA2 microscope equipped with an ORCA-ER chilled CCD camera (Hammamatsu) and the Openlab capture software (Improvision).

Indirect immunofluorescence

Cells grown on glass coverslips were treated with DNA damaging agents or transcription inhibitors as described in the figure legends, washed with PBS and fixed for 15 minutes either with 2% formaldehyde or 1% formaldehyde/0.1% Triton X-100 in ice-cold PBS. Cells were washed three times with ice-cold PBS/0.1% Triton X-100/0.5% BSA, then incubated overnight at 4°C with an affinity purified rabbit polyclonal anti-PARP-2 antibody (Yuc 1:200), a mouse monoclonal anti-B23 (1:2000, kindly given by P. K. Chan, Houston, TX) or an anti-PARP-1 ($C_{2\text{-}10}$, 1:200) antibodies. After three washes with ice-cold PBS/0.1% Triton X-100, cells were incubated for 3 hours at 4°C with Alexa Fluor 568 goat anti-rabbit IgG (1:2000, Molecular Probes) or Alexa Fluor 488 goat anti-mouse IgG (1:2000, Molecular Probes). DNA was counterstained with DAPI (25 ng/ml in PBS/0.1% Triton X-100). Cells were observed either as above for wide field views or with a Leica TCS4D confocal microscope equipped with an argon/krypton laser and suitable barrier filters.

Cellular fractionation, GST pull-down, immunoprecipitation and western blot analyses

HeLa cells (2×10^7 cells) were separated into cytoplasmic, nucleoplasmic and nucleolar fractions as described previously (Scherl et al., 2002). 15 μg of each fraction were analyzed by western blotting with the indicated antibodies. Immunoreactivity was detected by chemiluminescence (Amersham). For GST pull-down analyses, HeLa cells (5×10^5 cells) were transfected by calcium-phosphate coprecipitation with 10 μg recombinant DNA. 48 hours later, cells were lysed by two cycles of freeze/thaw in 400 mM KCl, 20 mM HEPES, pH 7.9, 20% Glycerol, 5 mM DTT, 0.5 mM EDTA, 0.5 mM PMSF and protease inhibitors (Complete Mini, Roche). When indicated, 4 mM 3-aminobenzamide (3-AB) was added to the culture medium 3 hours before lysis and maintained throughout the experiment. Treatment with actinomycin D (0.2 μg/ml) was performed 3 hours before lysis. Lysates were clarified by centrifugation and diluted to obtain the following concentrations: 150 mM KCl, 20 mM HEPES pH 7.9, 0.2% NP-40, 0.5 mM EDTA, 0.5 mM PMSF. When indicated, 10 μg/ml ethidium bromide or 4 mM 3-AB were added. For GST pull down, lysates were incubated for 3 hours with glutathione-Sepharose beads (Pharmacia). For immunoprecipitation, lysates were precleared for 30 minutes with Protein G-Sepharose beads, then incubated for 3 hours with 5 μg monoclonal anti-GFP antibody (Roche) and for 1 hour with Protein-G-sepharose beads. Beads and co-purified proteins were washed three times with 150 mM KCl, 20 mM HEPES pH 7.9, 0.2% NP-40, 0.5 mM EDTA, 0.5 mM PMSF eventually supplemented with 4 mM 3-AB or 10 μg/ml ethidium bromide. Samples were resuspended in Laemmli buffer, boiled for 4 minutes and analyzed by 10% SDS-PAGE and western blot. Blots were incubated with mouse monoclonal anti-B23 (1:10,000) and anti-GST (1:10,000, IGBMC, Illkirch, France) antibodies or rabbit polyclonal anti-GFP (1:1000) antibodies. Blots were then probed with horseradish peroxidase-coupled goat anti mouse antibody (1:4000, Sigma), and immunoreactivity was detected by chemiluminescence (Amersham). For PARP-1 and PARP-2 immunodetection, cells were resuspended in Laemmli buffer, sonicated and 2×10^5 cells were analyzed by western blotting with a mouse polyclonal anti PARP-1 antibody (EGT69, 1:10,000) or a rabbit polyclonal anti-PARP-2 antibody (1:4000, Alexis).

Northern Blot

Total RNAs were extracted from cells grown in 6 cm plates by the single-step procedure (Chomczynski and Sacchi, 1987) using guanidinium isothiocyanate.

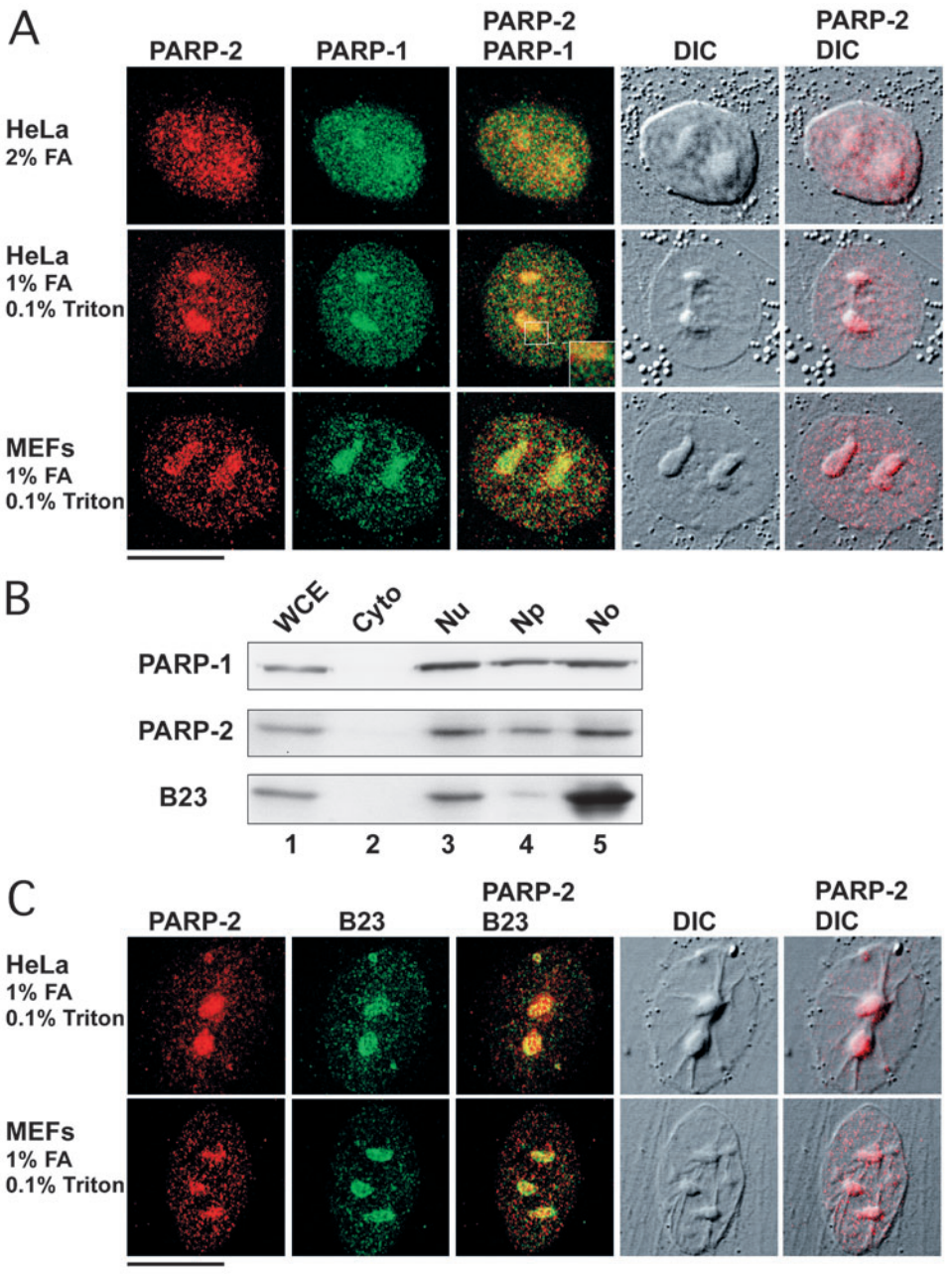

Fig. 1. Subnuclear distribution of endogenous PARP-2 in human and mouse cells. (A) Confocal sections showing the simultaneous immunodetection of PARP-2 and PARP-1 in HeLa cells fixed with 2% formaldehyde (FA, top), or HeLa cells (middle) and MEFs (bottom) fixed with 1% formaldehyde/0.1% Triton X-100. The morphology of the nucleus is illustrated by differential interference contrast (DIC) images. Merged images of stained PARP-2 and either stained PARP-1 or the DIC image are shown. Inset shows a 2× magnification of the area indicated by the square. To improve the resolution of final images, only the nuclei are displayed as no specific signal above background was detected in the cytoplasm. (B) Cellular fractionation of HeLa cells. 15 μg of each cellular fraction were analyzed by western blotting with antibodies against B23 (bottom), PARP-2 (middle) and PARP-1 (top). WCE, whole cell extract; Cyto, cytoplasmic fraction; Nu, nuclear fraction; Np, nucleoplasmic fraction; No, nucleolar fraction. (C) Confocal sections showing the simultaneous immunodetection of PARP-2 and B23 in HeLa cells (top) or MEFs (bottom) fixed with 1% formaldehyde/0.1% Triton X-100. Merged images of stained PARP-2 and either stained B23 or the DIC image are shown. Bar, 10 μm.

3 μg RNA were fractionated by electrophoresis on a 1% agarose gel in the presence of formaldehyde and transferred onto Hybond N filters (Amersham). The riboprobe corresponding to the 5′ end (nucleotides 1-155) of mouse pre-rRNA was generated by in vitro transcription of the *Bam*HI linearized pGem-3WT (kindly given by I. Grummt, Heidelberg, Germany) using the Riboprobe In Vitro Transcription System (Promega). Hybridization was carried out for 16 hours at 68°C in Dig Easy Hyb (Roche). Blots were subjected to autoradiography and phosphorimaging analysis for quantification (Biorad).

Results

PARP-2 accumulates within the nucleolus of mouse and human cells independently of PARP-1

The subcellular distribution of PARP-2 was compared with that of PARP-1 by indirect immunofluorescence and confocal laser-scanning microscopy in human cells (HeLa) fixed with 2% formaldehyde. PARP-2 and PARP-1 showed both a nuclear punctate distribution and a stronger accumulation into subnuclear structures identified as nucleoli by differential interference contrast (DIC) images (Fig. 1A, top row). Cell fixation with 1% formaldehyde in the presence of 0.1% Triton X-100 eliminated soluble proteins within the nucleoplasm, whereas the nucleolar fraction of PARP-2 and PARP-1 remained high, both in human HeLa cells (Fig. 1A, middle row) and mouse embryonic fibroblast cells (MEFs) (Fig. 1A, bottom row). To confirm the nuclear and nucleolar distribution of PARP-2 and PARP-1, HeLa cells were subfractionated and immunoblotted with anti-PARP-2 and anti-PARP-1 antibodies. As expected, PARP-2 and PARP-1 were present in the nucleoplasmic fraction and slightly more abundant in the nucleolar fraction (Fig. 1B). The immunodetection of B23 in the nucleolar fraction confirmed the integrity of the fractions. Taken together, these results indicate that PARP-2, like PARP-1 (Desnoyers et al., 1996; Fakan et al., 1988; Mosgoeller et al., 1996), is abundant in the nucleoplasm and accumulates within nucleoli in mammalian cells. This subcellular distribution is consistent with that observed in living cells for PARP-2 fused to GFP (see Fig. 4).

Interestingly, despite the fact that PARP-1 and PARP-2 display a similar subnuclear distribution pattern and were found to heterodimerize in vitro (Schreiber et al., 2002), the merged confocal images revealed that they do not strictly colocalize (Fig. 1A): partial colocalization was evident within nucleoli, whereas less overlap was evident within the nucleoplasm. Therefore, PARP-1 and PARP-2 share numerous common subcellular sites within the nucleolus but fewer within the nucleoplasm.

PARP-1 was reported to reside at least within the dense fibrillar component (DFC) (Fakan et al., 1988; Mosgoeller et al., 1996) and the granular component (GC) (Fakan et al., 1988). In order to determine whether PARP-2 localization is restricted to a particular nucleolar region, we co-stained HeLa cells (Fig. 1C, top row) or MEFs (Fig. 1C, bottom row) with anti-PARP-2 antibodies and several antibodies specific for nucleolar proteins such as B23 (Spector et al., 1984), fibrillarin (Masson et al., 1990) and Upstream Binding Factor (UBF) (Roussel et al., 1993). PARP-2 showed partial colocalization with all three nucleolar factors (Fig. 1C and data not shown) suggesting that the protein is present throughout the entire nucleolus. This is confirmed by the comparison of PARP-2 immunostaining with the DIC image that shows an overlap between PARP-2 intense labeling and phase-dense regions that define nucleoli (Fig. 1A and C).

As a control of the specificity of the anti-PARP-2 antibody, we verified the absence of detectable signal in MEFs from PARP-2$^{-/-}$ embryos. In PARP-1 deficient cells, we noticed that PARP-2 was still accumulated within the nucleolus (Fig. 2). Reciprocally, PARP-1 accumulated within the nucleolus in PARP-2 deficient cells. These observations indicate that despite their possible heterodimerization (Schreiber et al., 2002), PARP-1 and PARP-2 localize within the nucleolus independently of each other.

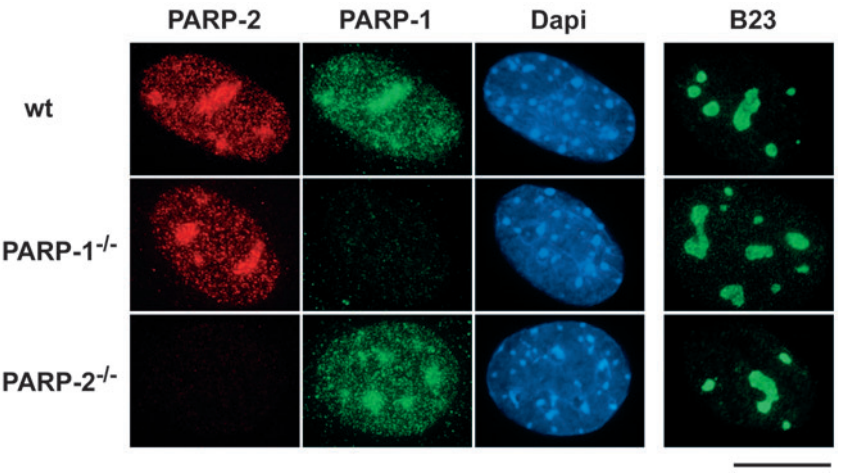

Fig. 2. PARP-1 and PARP-2 accumulate in the nucleolus independently of each other. Wide-field views of the simultaneous immunodetection of PARP-2 and PARP-1 in wild type (top), PARP-1$^{-/-}$ (middle) and PARP-2$^{-/-}$ (bottom) MEFs fixed with 1% formaldehyde/0.1% Triton X-100. DNA is stained with DAPI. Co-immunodetection of PARP-2 and B23 was performed in parallel under the same conditions, only the B23 staining is shown in the right column. Bar, 10 μm.

Characterization of the nuclear and nucleolar localization determinants of mouse PARP-2

To gain an insight into the determinants required for the nucleolar accumulation of murine PARP-2, we cloned partial cDNA fragments in-frame with the C-terminus of the enhanced green fluorescent protein (GFP; Fig. 3). In order to circumvent any misinterpretation of the subcellular localization of the recombinant proteins that may be altered during the fixation procedure, we chose to follow the distribution of the GFP-tagged polypeptides in living PARP-2$^{-/-}$ MEFs. The use of PARP-2$^{-/-}$ cells prevents the nucleolar accumulation via homodimerization with endogenous PARP-2 (Schreiber et al., 2002). GFP alone was homogeneously diffused within the whole cell, but the nucleoli were excluded (Fig. 3a). The NLS of SV40-T antigen (residues 125-136) (Kalderon et al., 1984) fused to GFP was able to target the recombinant protein into the nucleus, but not into the nucleolus (Fig. 3b). When necessary, this SV40-T antigen NLS was inserted in-frame

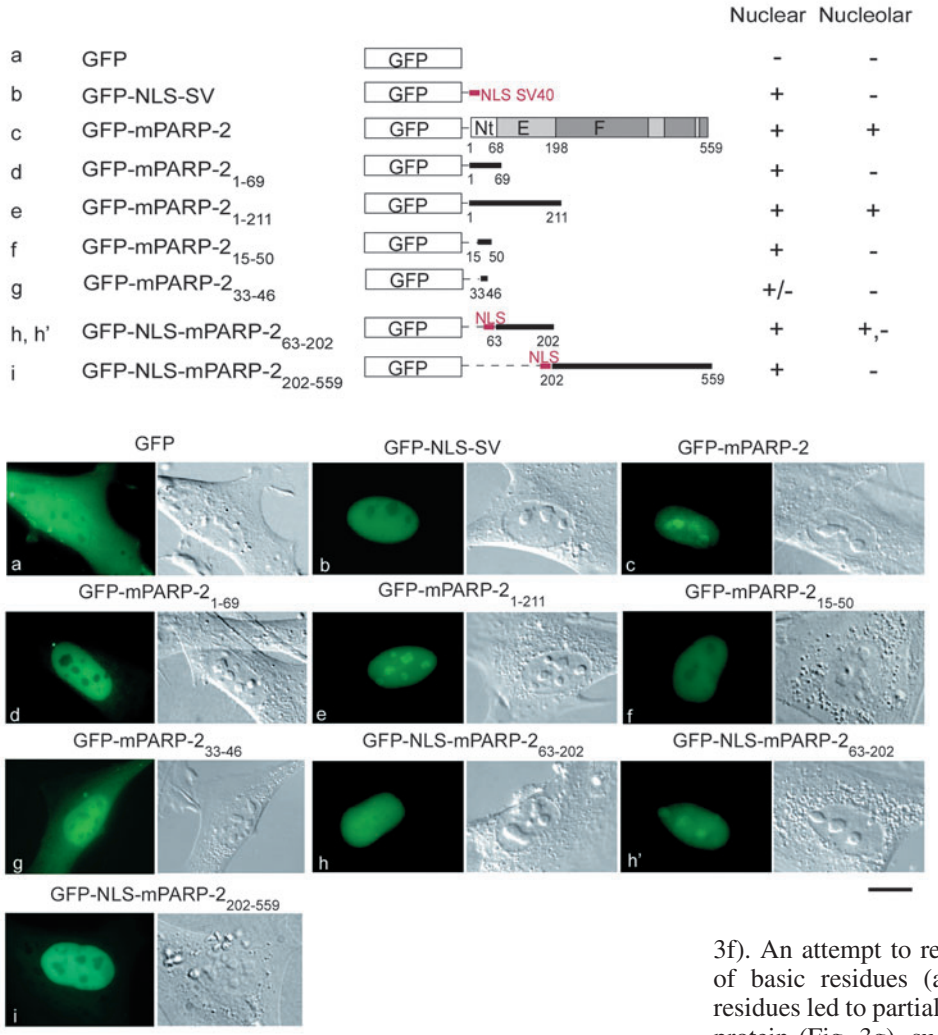

Fig. 3. Localization in living PARP-2$^{-/-}$ MEFs of full-length and truncated versions of mouse PARP-2 fused to the C-terminus of GFP. (Top) Schematic representation of mPARP-2 or truncated versions of mPARP-2 fused to GFP. When indicated, the NLS of SV40-T was inserted in frame between the coding sequence of GFP and the sequence from mPARP-2. Fusion proteins were present (+) or not (–) in the nucleus or the nucleolus. (Bottom) Localization in living PARP-2$^{-/-}$ MEFs of the GFP-fused recombinant proteins (left panels) labelled as in the scheme above. The corresponding DIC images are shown on the right. Bar, 10 μm.

between GFP and the PARP-2 polypeptides to target the recombinant proteins to the nucleus. Murine PARP-2 fused to GFP displayed a similar subcellular distribution as that observed by immunofluorescence with anti-PARP-2 antibodies (Fig. 1): the recombinant protein accumulated in the nucleus and the nucleolus (Fig. 3c), thus validating the experimental approach. Interestingly, the N-terminal domain of mouse PARP-2 (Nt; residues 1-69, encompassing the DNA binding domain) fused to the C-terminus of GFP could enter the nucleus but remained excluded from the nucleolus (Fig. 3d). The E domain of murine PARP-2 (residues 63-202) could not accumulate in the nucleus (data not shown) unless the NLS of SV40-T antigen was present (Fig. 3h,h′). In this situation, the recombinant protein showed a homogeneous nuclear distribution (Fig. 3h) with 27% of cells showing an accumulation in the nucleolus (Fig. 3h′). The fusion protein harboring both the Nt and the E domains of murine PARP-2 (residues 1-211) was predominantly nucleolar (Fig. 3e), suggesting that the presence of both domains is required for efficient nucleolar targeting. The catalytic F domain of murine PARP-2 (residues 202-559) which could not reach the nucleus by itself (data not shown) remained excluded from the nucleolus even in the presence of the SV40-T antigen NLS (Fig. 3i).

Taken together, these results indicate that the Nt domain of murine PARP-2 contains the NLS responsible for the nuclear localization of the whole protein, as it is the only polypeptide capable of directing the GFP to the nucleus. The primary sequence of this DNA binding domain revealed the presence of two stretches of basic amino acids (KK_{20}-X_{15}-$KKMRTCQRK_{44}$) that could resemble a bipartite NLS (Schreiber et al., 1992). Indeed, this polypeptide was able to target GFP into the nucleus, not into the nucleolus (Fig. 3f). An attempt to restrict this sequence into a unique stretch of basic residues (amino acids 33-46) flanked by proline residues led to partial nuclear accumulation of the recombinant protein (Fig. 3g), suggesting that this sequence needs the N-terminal flanking basic stretch to function efficiently as a NLS.

There is no established consensus for NoLSs, although they are frequently enriched in arginine and lysine residues. Analysis of the primary sequence of human and murine PARP-2 revealed the presence of an arginine-rich sequence (residues 4-7) in the extreme N-terminus of the DNA binding domain, whereas both the E and the F domains were devoid of such basic sequences. Therefore, the fact that the Nt domain of mouse PARP-2 fused to the C-terminus of GFP failed to accumulate within the nucleolus was unexpected. As this stretch of arginines differs between human and murine PARP-2, we wondered whether the human Nt domain could accumulate in the nucleolus when fused to the C-terminus of GFP. The recombinant protein accumulated within the nucleolus (Fig. 4c) similar to full-length human PARP-2 fused to GFP (Fig. 4a). Therefore, although the Nt domain of human PARP-2 harbors a functional NoLS, the Nt domain of murine PARP-2 may encounter a folding problem when fused to the C-terminus of GFP. To validate this possibility, the Nt domain of murine PARP-2 was fused in frame with the N-terminus of GFP. As expected, the recombinant protein accumulated within the nucleolus (Fig. 4e). This was also the case for the Nt domain of human PARP-2 or full-length mouse PARP-2, both fused to the N-terminus of GFP (Fig. 4d and b, respectively). Together, these results demonstrate that the Nt domain of

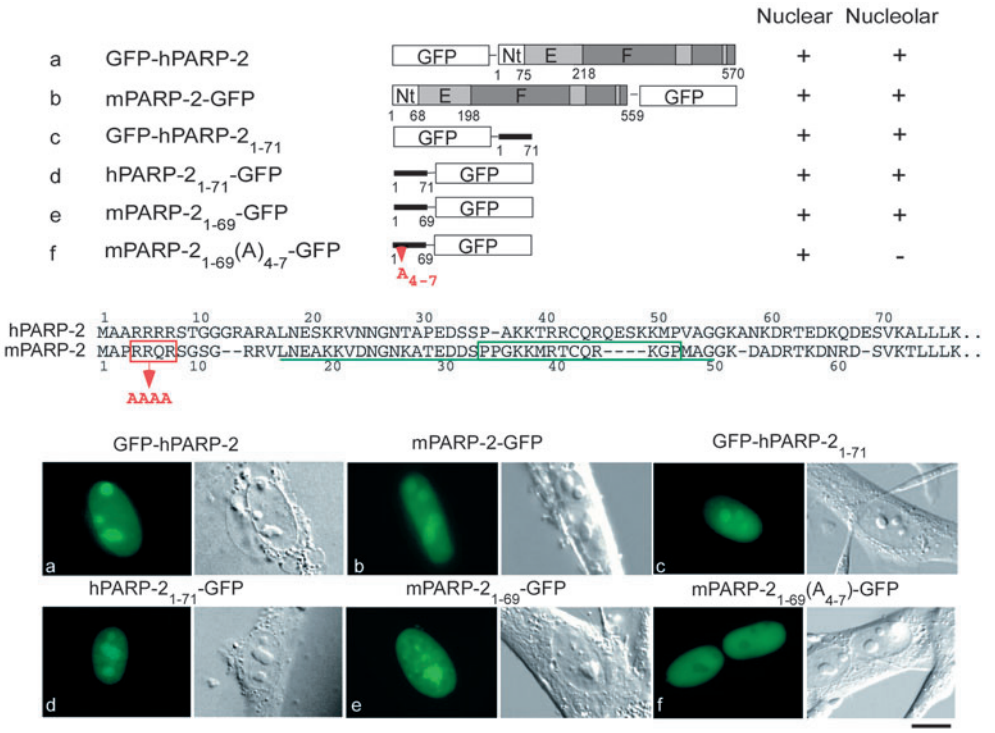

Fig. 4. Identification of the NoLS of mouse PARP-2. (Top) Schematic representation of the recombinant proteins, as described in Fig. 3. The substitution of 4-RRQR-7 to four alanines is indicated in red. Residues 15-50 and 33-46, involved in nuclear targeting, are underlined or boxed in green, respectively. (Bottom) Localization in living PARP-2$^{-/-}$ MEFs of the GFP-fused recombinant proteins (left panels) each labelled as in the scheme above. The corresponding DIC images are presented on the right. Bar, 10 μm.

PARP-2 possesses a functional NoLS that, for its murine counterpart seems susceptible to its structural context when fused to the reporter protein GFP. In order to determine whether the stretch of arginines is involved in the NoLS, residues 4-7 were mutated to alanines in the Nt of mouse PARP-2 fused to the N-terminus of GFP. As shown in Fig. 4f, these mutations abolished the nucleolar localization of the recombinant protein, while maintaining its nuclear localization. Therefore, the NoLS of PARP-2 encompasses this stretch of arginines in the extreme N-terminus of the protein.

PARP-1 and PARP-2 interact with B23

PARP-1 was reported to co-purify with the nucleolar factor B23, and B23 was found to be poly(ADP-ribosyl)ated following γ irradiation (Borggrefe et al., 1998; Leitinger and Wesierska-Gadek, 1993; Ramsamooj et al., 1995). Therefore, we wondered whether PARP-2 could also associate with B23. Fusion proteins made of GST and murine PARP-2 (GST-mPARP-2), human PARP-2 (GST-hPARP-2) or human PARP-1 (GST-hPARP-1) were overexpressed in HeLa cells and interacting proteins were analyzed by GST pull-down experiments followed by western blotting (Fig. 5A). B23 co-purified with GST-hPARP-1 (Fig. 5A, lane 2) and GST-hPARP-2 (Fig. 5A, lane 8) or GST-mPARP-2 (Fig. 5B, lane 10) but not with GST alone (Fig. 5A, lanes 7 and Fig. 5B, lanes 2 and 9) demonstrating that B23 interacts with both PARPs.

We next examined the conditions regulating the association between PARP-1, PARP-2 and B23 (Fig. 5A). To analyze the effect of poly(ADP-ribosyl)ation reactions, HeLa cells expressing either GST-hPARP-1 or GST-hPARP-2 were left untreated (lanes 2, 5, 8 and 11), treated for 10 minutes with 1 mM H_2O_2 to stimulate poly(ADP-ribose) synthesis (lanes 3 and 9), or preincubated for 3 hours with either 4 mM 3-aminobenzamide (3-AB) to inhibit PARP activity (lanes 4 and 10) or with 0.2 μg/ml actinomycin D to inhibit RNA pol I transcription (lanes 6 and 12). Proteins were analyzed by GST pull-down experiments and western blotting by successively probing with the indicated antibodies (Fig. 5A). Results showed that the association of B23 with either PARP-1 or PARP-2 is not dependent on poly (ADP-ribosyl)ation (compare lanes 4 and 10 with 2 and 8). To prevent any co-purification of both proteins through DNA, ethidium bromide was added throughout the pull down in some samples (lanes 5 and 11). This had no effect on co-purification of B23 with either GST-fused PARP, indicating that DNA is not involved in the interaction of PARP-1 and PARP-2 with B23. In addition, transcription of rRNAs is not a prerequisite for the interaction between these protein partners as its inhibition by actinomycin D (or camptothecin, data not shown) had no consequences on the co-purification efficiencies.

To map the B23 interaction domains within PARP-1 and PARP-2, GST pull-down experiments were performed with fusion proteins made of GST and truncated versions of either hPARP-1 (Fig. 5B, lanes 3-7) or mPARP-2 (lanes 11-13). Co-purification of B23 was efficient with the recombinant proteins containing the N-terminal DNA binding domain of mPARP-2 (GST-mPARP-2_{1-69}, lane 11) and, more weakly, with GST-mPARP-2_{63-202} (lane 12) that contains the homodimerization E domain (Schreiber et al., 2002). This weak co-purification of B23 observed with the E domain of PARP-2 could be due to the interaction between GST-mPARP-2_{63-202} and endogenous PARP-2, the latter being able to trap B23 via its N-terminal DNA binding domain. Regarding PARP-1, B23 was found to co-purify with GST-hPARP-1_{1-371} (lane 3) and GST-hPARP-$1_{384-524}$ (lane 5) harboring respectively the DNA binding (A) domain and the BRCT (D) domain of hPARP-1, both already described as platforms for protein-protein interaction with several partners, notably XRCC1, DNA pol β, DNA ligase III (Schreiber et al., 2002). Taken together, these results demonstrate that PARP-1 and PARP-2 interact constitutively with B23 through the DNA binding domain of PARP-2 and the DNA binding and BRCT domains of PARP-1.

We then wondered whether the mutation of residues 4-7 of mPARP-2, which abolishes nucleolar accumulation of the Nt

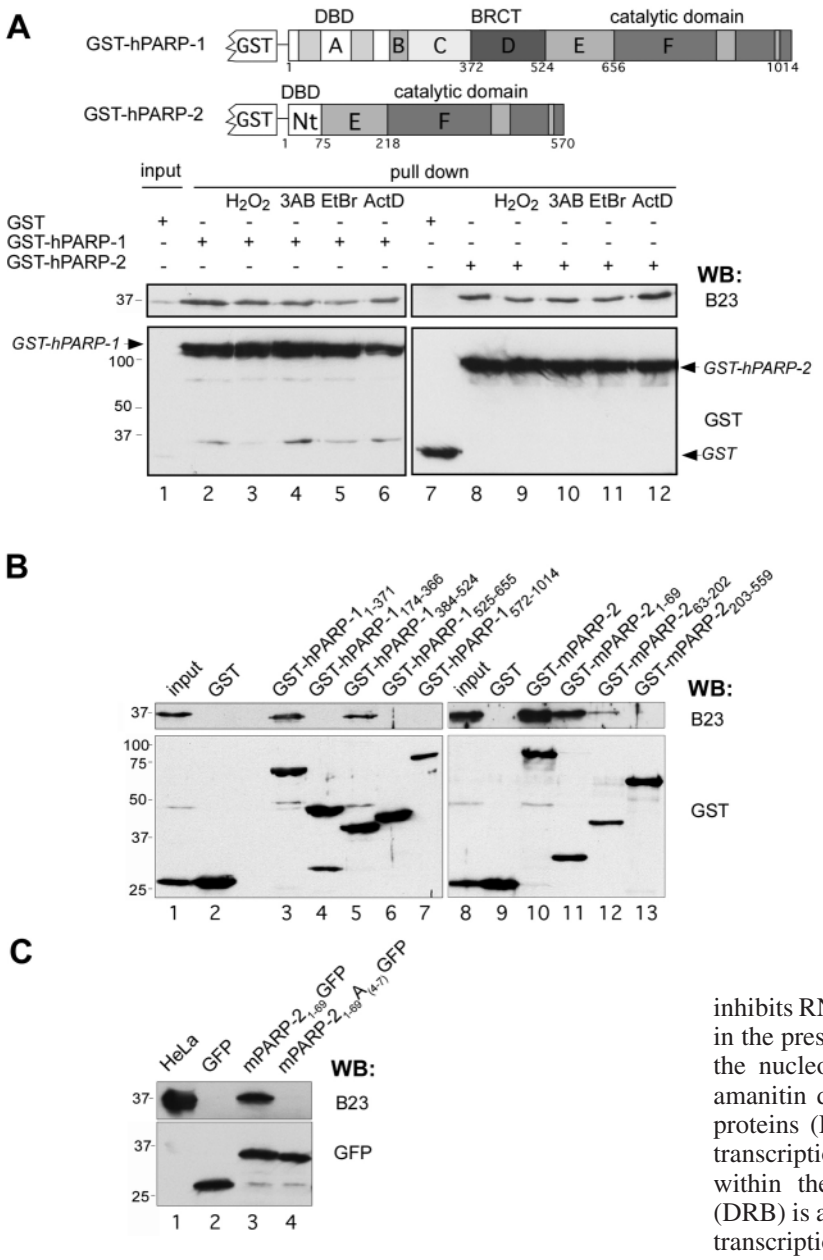

Fig. 5. B23 interacts constitutively with PARP-1 and PARP-2 through their DNA binding domains and PARP-1 BRCT domain. (A) Schematic representation of GST-hPARP-1 and GST-hPARP-2. DBD, DNA binding domain. GST (lane 7), GST-hPARP-1 (lanes 2-6) or GST-hPARP-2 (lanes 8-12) were overexpressed in HeLa cells either untreated (lanes 2, 5, 8 and 11) or treated with 1 mM H_2O_2 for 10 minutes (lanes 3 and 9), 4 mM 3-AB for 3 hours (lanes 4 and 10) or 0.2 μg/ml actinomycin D for 3 hours (ActD, lanes 6 and 12). 10 μg/ml ethidium bromide was added to the lysate (EtBr, lanes 5 and 11). Proteins were analyzed by GST pull down and western blot using anti-B23 and anti-GST antibodies as indicated in the lower panel. Lane 1: input corresponding to 1/30th of the lysate. (B) GST (lanes 2 and 9), GST mPARP-2 (lane 10) or GST-tagged deletion mutants of hPARP-1 (lanes 3-7) or of mPARP-2 (lanes 11-13) were expressed in HeLa cells. Interacting proteins were analyzed by GST pull down and western blotting with anti-B23 and anti-GST antibodies. Input (lanes 1 and 8): 1/30th of the GST-expressing cell lysate. (C) Immunoprecipitation with anti-GFP antibodies of GFP (lane 2), mPARP-$2_{1\text{-}69}$-GFP (lane 3) and mPARP-$2_{1\text{-}69}A_{4\text{-}7}$GFP (lane 4) overexpressed in HeLa cells. Western blots were subsequently probed with a monoclonal anti-B23 antibody (top) and a polyclonal anti GFP antibody. Lane 1: crude extract from 10^5 HeLa cells.

domain fused to the N-terminus of GFP, affects the binding to B23. GFP, mPARP-$2_{1\text{-}69}$-GFP or mPARP-$2_{1\text{-}69}A_{4\text{-}7}$-GFP transiently overexpressed in HeLa cells were immunoprecipitated with anti-GFP antibodies and co-purification of B23 was assessed by western blot analyses (Fig. 5C). B23 efficiently co-purified with mPARP-$2_{1\text{-}69}$-GFP (lane 3) but not with mPARP-$2_{1\text{-}69}A_{4\text{-}7}$-GFP (lane 4), demonstrating the importance of a functional NoLS not only for nucleolar localization but also for binding to B23.

PARP-2 is delocalized from the nucleolus upon RNA pol I transcription inhibition

It has been shown that the nucleolar localization of PARP-1 requires active transcription (Desnoyers et al., 1996), but whether it was RNA pol I or RNA pol II transcription was not clarified. In order to determine whether PARP-1 and PARP-2 nucleolar accumulation depends on nuclear or nucleolar transcription, we performed indirect immunofluorescence analyses on primary MEFs 2 hours after treatment of cells with 0.05 μg/ml actinomycin D or 50 μg/ml α-amanitin (Fig. 6). At these doses, actinomycin D is known to specifically inhibit RNA pol I, whereas α-amanitin inhibits RNA pol II (Perry and Kelley, 1970). We observed that, in the presence of actinomycin D, PARP-2 is delocalized from the nucleolus, together with PARP-1 and B23, whereas α-amanitin did not disrupt the nucleolar accumulation of these proteins (Fig. 6). These results suggest that active nucleolar transcription is required for PARP-1 and PARP-2 to reside within the nucleolus. Dichlororibofuranosyl benzimidazole (DRB) is a compound that unravels and disperses the nucleolar transcription units within the nucleus, without abolishing their transcription (Panse et al., 1999). When cells were treated for 1 hour with DRB, PARP-1, PARP-2 and B23 followed this typical dispersion within the nucleus (Fig. 6). This dispersion was reversible, as removal of the DRB and subsequent incubation for 1 hour in fresh medium allowed the relocalization of PARP-1, PARP-2 and B23 within the nucleolus. When cells were treated with 10 μM camptothecin for 30 minutes, PARP-1, PARP-2 and B23 were also delocalized from the nucleolus (Fig. 6). At this dose, this topoisomerase I inhibitor completely inhibits RNA pol I transcription (see Fig. 8). Interestingly, the camptothecin-induced nucleolar delocalization of PARP-1, PARP-2 and B23 does not require the activation of PARPs, as it is still observed in the presence of 3-AB, as well as in the PARP-1 or PARP-2 knockout MEF (data not shown). Taken together, these results indicate that PARP-1 and PARP-2 accumulation within nucleoli of murine and human cells is dependent upon active transcription of nucleolar RNAs by RNA pol I.

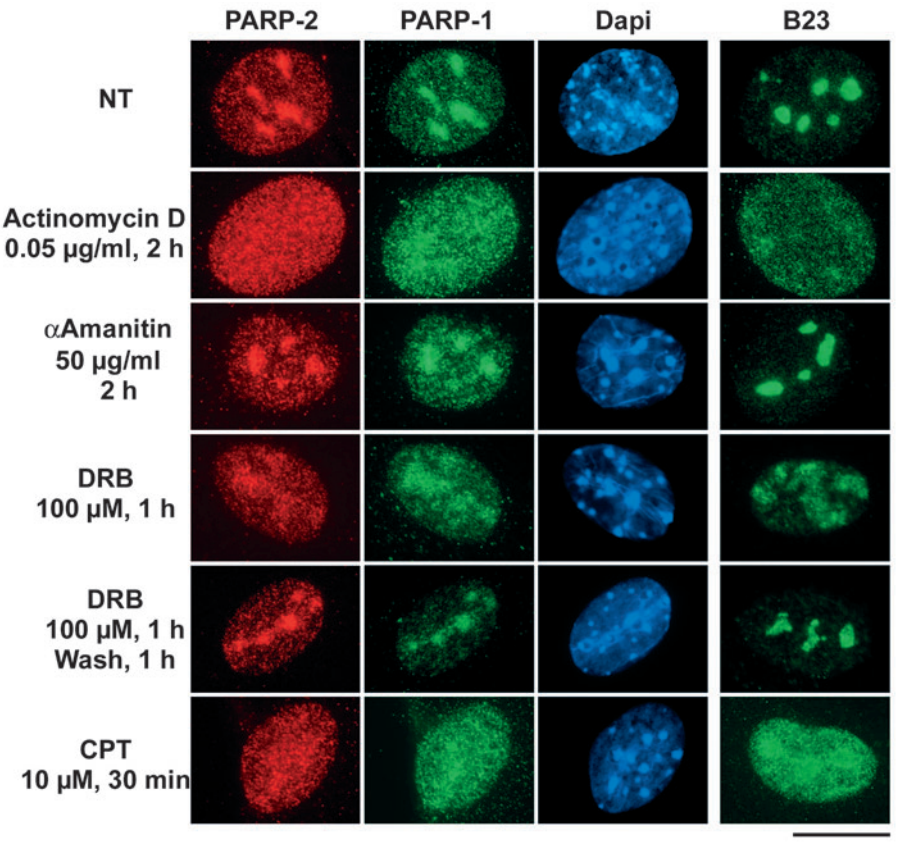

Fig. 6. PARP-1 and PARP-2 are delocalized from the nucleolus upon RNA pol I transcription inhibition. Wide field views of the simultaneous immunodetection of PARP-2 and PARP-1 in wild-type MEFs treated or not (NT, not treated) with 0.05 µg/ml actinomycin D for 2 hours, 50 µg/ml α-amanitin for 2 hours, 100 µM DRB for 1 hour, and in one experiment, followed by two washes with PBS and a 1 hour incubation in fresh medium or 10µM camptothecin (CPT) for 30 minutes. Cells were fixed with 1% formaldehyde/0.1% Triton X-100. DNA is stained with DAPI. Co-immunodetection of PARP-2 and B23 was performed in parallel under the same conditions; only the B23 staining is shown in the right panels. Bar, 10 µm.

The nucleolar accumulation of PARP-1, PARP-2 and B23 is only moderately affected by alkylated or oxidative DNA damage

The DNA damage-dependent PARP-1 and PARP-2 are activated by the presence of DNA strand breaks resulting from treatment of cells with hydrogen peroxide or methyl methane sulfonate (MMS). In order to determine whether DNA damage affects the nucleolar localization of PARP-1 and PARP-2, we treated wild-type MEFs with increasing doses (0.2, 0.5, 1 and 2 mM) of H_2O_2 or MMS for 10 minutes to 2 hours. The subcellular localization of both PARPs, as well as that of B23, is only moderately affected by lethal doses of H_2O_2 or 2 mM MMS (Fig. 7A and data not shown). Lower doses (200 µM), although sufficient to generate DNA lesions that strongly activate poly(ADP-ribose) synthesis and require several hours for complete repair (Trucco et al., 1998), had no effect on PARP subcellular distribution. Treatment for 1 hour with 1 µg/ml 4-nitroquinoline 1-oxide (4NQO), another PARP-activating agent (Yu et al., 1986), leads to the extinction of PARP-1, PARP-2 and B23 nucleolar staining (Fig. 7A). Bulky adducts are generated by 4NQO on DNA and, like camptothecin, it inhibits transcription (Gray et al., 1998 and see below), whereas H_2O_2 and MMS have lesser blocking effects on RNA pol I transcription (see below). Therefore, the nucleolar accumulation of PARP-1 and PARP-2 is affected by transcription inhibition rather than by DNA lesions that do not radically disrupt RNA pol I transcription.

The moderate decrease of the nucleolar localization of PARP-1 and PARP-2 observed when cells were treated with high doses of alkylating or oxidizing DNA damaging agents could result from proteolytic cleavage of the proteins, as proposed (Alvarez-Gonzalez et al., 1999). As PARP-1 and PARP-2 are cleaved during apoptosis by the apoptotic caspase-3 (Kaufmann et al., 1993; Menissier de Murcia et al., 2003), we examined by western blotting whether the integrity of the two proteins was affected by any of the cell treatments performed to affect the nucleolar retention of PARP-1 and PARP-2 (Fig. 7B). Interestingly, neither PARP-1 nor PARP-2 were cleaved in any of the conditions examined. These results indicate that the dramatic drop of PARP-1 and PARP-2 nucleolar staining observed when RNA pol I transcription is inhibited (by actinomycin D, camptothecin, 4NQO) as well as the moderate delocalization upon high doses of H_2O_2 or MMS, does not result from proteolytic cleavage of the two proteins.

Normal transcription of ribosomal RNA in PARP-1 or PARP-2 deficient cells

The dependence on effective nucleolar transcription for the nucleolar accumulation of PARP-1 and PARP-2 suggests that they may somehow be involved in the process of rRNA transcription. This hypothesis prompted us to check whether the absence of one or other PARP or their chemical inhibition in MEFs had repercussions on rRNA transcription. The 47S pre-rRNA transcription was monitored by northern blotting of cell lysates derived from wild type, PARP-$1^{-/-}$ or PARP-$2^{-/-}$ MEFs treated or not with MMS (200 µM, 2 hours), H_2O_2 (200 µM, 2 hours), camptothecin (10 µM, 1 hour) or 4NQO (1 µg/ml, 1 hour) in the presence or absence of 3-AB (Fig. 8). The probe used was specific of the pre-rRNA, as it hybridized to the 5′ extremity of the pre-rRNA, a region that is eliminated by the first step of maturation. Results indicate that transcription of the pre-rRNA occurs at similar levels regardless of the genotype and is not affected by treatment with alkylating or oxidizing agents. Camptothecin and 4NQO completely inhibited pre-rRNA transcription, but for all three genotypes. The abundant smaller-sized RNAs observed upon cell treatment with camptothecin could be interpreted as a block of elongation when the transcription machinery is stopped by trapped topoisomerase I cleavage complexes at topoisomerase I binding sites (Fig. 8). With 4NQO, we

hypothesized that the abundant smaller-sized RNAs are produced by abortive transcription elongation when the transcription machinery encounters a 4NQO-induced bulky adduct. Taken together, our results indicate that the absence of PARP-1 or PARP-2 or inhibition of their catalytic activity does not affect nucleolar transcription of ribosomal RNAs.

Discussion

PARP-2, like PARP-1, accumulates within mammalian cell nucleoli

In this study, we demonstrate that PARP-2, like PARP-1, is enriched within the nucleolus. The nucleolar accumulation of PARP-2 was observed in all human cell lines tested (HEK293, MRC5, human diploid fibroblasts) but also in mouse cells and was observed throughout the cell cycle, as long as the nucleoli were not disorganized during mitosis (data not shown). We have shown previously that PARP-1 and PARP-2 can heterodimerize in vitro, demonstrating a direct contact between them (Schreiber et al., 2002). An unexpected finding of the present study was that PARP-1 and PARP-2 nuclear distributions were not totally overlapping. Although both proteins accumulated in the nucleolus independently of one another, confocal analyses revealed that they only partially colocalize there. Colocalization was even weaker in the nucleoplasm. This unexpectedly low colocalization was also observed upon cell treatment with the DNA-damaging agents MMS and H_2O_2, which both trigger poly(ADP-ribose) synthesis at damaged sites. We hypothesize that PARP-1 and PARP-2 may have distinct targets and/or distinct subcellular sites within the nucleus and their heterodimerization may be restricted to the nucleolus. If so, the biological function of this nucleolar heterodimerization remains to be determined.

The Nt DNA-binding and protein-binding domain of PARP-2 harbors a NLS and a NoLS

In this study, we have determined that the NLS and the NoLS of PARP-2 are confined to its Nt domain. An arginine-rich motif encompassing residues 4-7 is essential to target the mouse PARP-2 Nt domain to the nucleolus. This NoLS is functional when the Nt domain of mouse PARP-2 is fused by its C-terminus to GFP, but not when it is fused by its N-terminus. In the latter case, structural constraints may have affected the conformation of the NoLS. However, full-length mPARP-2 or the construct lacking only the catalytic domain, when fused to the C-terminus of GFP, were both able to reach the nucleolus. In both cases, the presence of the flanking E domain may have stabilized the

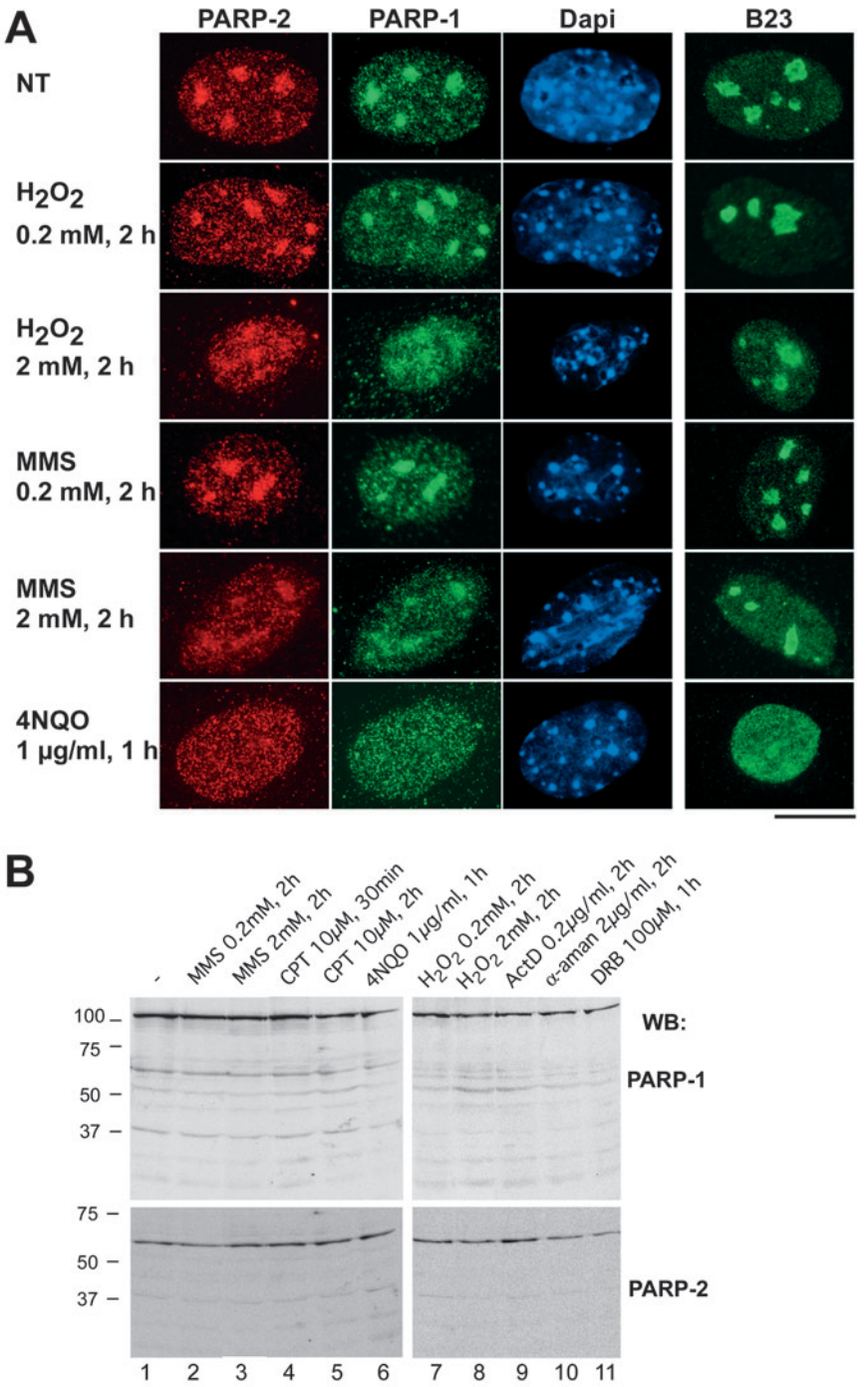

Fig. 7. PARP-1 and PARP-2 are only moderately delocalized from the nucleolus upon alkylated or oxidative DNA damage. (A) Wide field views of the immunodetection of PARP-2 and PARP-1 in wild-type MEFs treated or not (NT, not treated) with H_2O_2 (0.2 or 2 mM for 2 hours), MMS (0.2 or 2 mM for 2 hours) or 1 µg/ml 4NQO for 1 hour. Cells were fixed with 1% formaldehyde/0.1% Triton X-100. DNA is stained with DAPI. Co-immunodetection of PARP-2 and B23 in MEF cells treated in the same conditions. Only the B23 staining is shown in the panels on the right. (B) Western blot analyses with anti-PARP-1 or anti-PARP-2 antibodies performed on crude extracts of 2.5×10^5 MEFs submitted to the indicated treatments or not treated (–). Bar, 10 µm.

NoLS sequence through modification of the sterical constraints and/or via homodimerization of the recombinant proteins. In addition, when fused to the N-terminus of GFP, mPARP-2 accumulated more strongly in the nucleolus than when fused to the C-terminus of GFP. This was also the case for the Nt domain of hPARP-2. Therefore, the NoLS of both murine and human PARP-2 is more efficient when the N-terminus is free.

Altogether, our results demonstrate that the small Nt domain of PARP-2 encompassing the first 64 amino acids represents a multifunctional platform involved in nuclear and nucleolar targeting (this study), DNA binding (Amé et al., 1999), and protein/protein interactions (with B23 or with TRF2) (Dantzer et al., 2004). This domain is also released upon cleavage by caspase 3 during apoptosis (Menissier de Murcia et al., 2003).

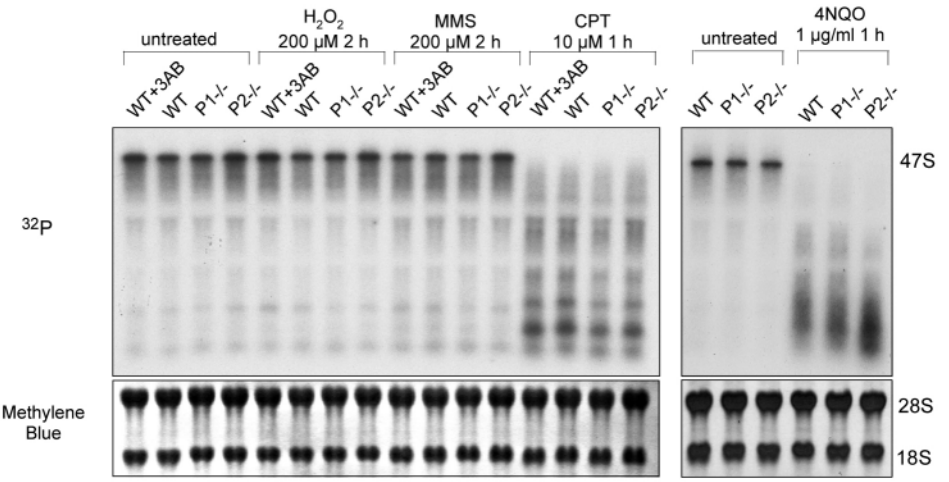

Fig. 8. The absence or inhibition of PARP-1 and PARP-2 has no repercussion on nucleolar transcription. Northern blot analysis of total RNAs obtained from the wild type (WT), PARP-$1^{-/-}$ (P1–/–), PARP-$2^{-/-}$ (P2–/–) or wild-type MEFs cultivated for 2 hours in the presence of 5 mM 3-AB (WT+3AB). Cells were either treated or not with the indicated agents. A typical experiment is illustrated. The upper panel shows the autoradiogram after hybridization of a 47S pre-rRNA specific probe; lower panel, staining of the membrane with methylene blue, showing the 28S and 18S rRNA as a loading control.

PARP-1 and PARP-2 interact with B23 in vivo and in vitro

We have shown here that PARP-1 and PARP-2 interact constitutively with the nucleolar factor B23, and neither of the cell treatments that totally or moderately affect their nucleolar accumulation disrupted their association. Mutation of the NoLS in mPARP-2 Nt domain abolished binding to B23. It is unlikely that this mutation affects the folding of the entire Nt domain as the NLS was still functional. It is more probable that either PARP-2 needs to be nucleolar in order to interact with B23, or PARP-2 is recruited to the nucleolus through binding to B23. B23 has been shown to have multiple functions: it is involved in ribosomal assembly; it is an endoribonuclease that cleaves the pre-ribosomal RNA (Savkur and Olson, 1998); it acts as a molecular chaperone (Szebeni and Olson, 1999); and is a regulator of cell proliferation, differentiation and apoptosis (Feuerstein et al., 1988; Liu and Yung, 1998). It has also been proposed that the stability and transcriptional activity of p53 is regulated by B23 (Colombo et al., 2002). The finding that B23 is poly(ADP-ribosyl)ated following γ irradiation (Leitinger and Wesierska-Gadek, 1993; Ramsamooj et al., 1995) suggests that the DNA-dependent PARPs and B23 could act together in the DNA damage-response pathway (see below).

The nucleolar accumulation of PARP-1 and PARP-2 depends on active RNA pol I transcription, but PARP-1 and PARP-2 are not required for nucleolar transcription

Our results show that the nucleolar accumulation of PARP-1 and PARP-2 requires active transcription of ribosomal RNAs by RNA pol I as both PARPs leave the nucleolus when transcription is inhibited either by actinomycin D, camptothecin or 4NQO. DNA damaging agents that have no evident blocking effects on nucleolar transcription, such as H_2O_2 or MMS, do not induce a massive delocalization of PARP-1 and PARP-2 from the nucleolus. In addition, we have verified that in all the situations where PARP-1 and PARP-2 appeared to move out of the nucleolus, this was not the result of their proteolytic cleavage, a phenomenon described earlier (Alvarez-Gonzalez et al., 1999). This discrepancy may come from the different cell type as well as DNA damaging agents used in both studies.

Our observations are reminiscent to those found with WRN: WRN is only partially delocalized upon treatment with H_2O_2, even at lethal doses, whereas 4NQO and camptothecin induce the extinction of detectable nucleolar WRN (Gray et al., 1998). The proliferation-dependent nucleolar antigen pKi-67 also translocates from nucleolus to nucleoplasm upon UV irradiation or 4NQO treatment, but not following H_2O_2 treatment (Al-Baker et al., 2004).

The interconnection between nucleolar accumulation and active RNA pol I transcription has been described previously for numerous factors, notably WRN or CSB, also delocalized from the nucleolus upon RNA pol I transcription inhibition. But although cells lacking WRN or CSB show an important reduction of rRNA transcription rate (Bradsher et al., 2002; Shiratori et al., 2002), cells lacking either PARP-1 or PARP-2 or where PARP activity is inhibited are not impaired in their rRNA transcription efficiency. This suggests that PARP-1 and PARP-2 are not directly involved into the nucleolar transcriptional process. However, previous in vitro studies have shown that PARP-1 could suppress non-specific transcription that may initiate at DNA breaks by RNA pol I, II and III (Kurl and Jacob, 1985; Slattery et al., 1983). In addition, the participation of PARP-1 as a co-factor in activation of RNA pol II-driven transcription of particular genes supports a function of PARP-1 in transcription (Kraus and Lis, 2003). In *Drosophila*, the disruption of PARP-1 expression, leading to larval lethality, revealed the importance of PARP-1 for the formation of nucleoli during development (Tulin et al., 2002).

Therefore, we cannot totally exclude the fact that PARP-1 and PARP-2 could play some redundant role in RNA pol I transcription. Such an overlapping function between retinoblastoma (Rb) family members in rRNA transcription explained the lack of effect of single inactivation of Rb, p107 or p130 genes on rRNA transcription, whereas $Rb^{-/-}p130^{-/-}$ double knockout cells displayed increased levels of ribosomal RNAs (Ciarmatori et al., 2001). Early embryonic lethality (at E7.5) was observed for the PARP-$1^{-/-}$PARP-$2^{-/-}$ double knockout mouse, highlighting some redundancy between PARP-1 and PARP-2 (Menissier de Murcia et al., 2003). Unfortunately, attempts to generate double knockout MEFs were not successful, preventing us from checking for a possible redundant function of PARP-1 and PARP-2 in rRNA transcription. However, we can assume that if PARP-1 and PARP-2 were simultaneously required for nucleolar transcription, this would not be through their catalytic activity as we show here that chemical inhibition of PARPs had no repercussion on transcription of the pre-rRNA.

What could be the function of PARP-1 and PARP-2 in the nucleolus?

The primordial function deciphered for PARP-1 and PARP-2 (DNA strand break detection and signaling) could account for their presence in the nucleolus as guardians of rDNA integrity. A striking observation we made is that poly(ADP-ribose) synthesis induced by oxidative or alkylating agents is less efficient in the nucleolus than in the nucleoplasm (data not shown). However, it has been shown that alkylated bases in the rDNA are efficiently repaired (Stevnsner et al., 1993), thus reflecting a proficient nucleolar base excision repair process.

One way to deal with DNA strand breaks is to set up recombination repair. The highly repetitive nature of rDNA makes it prone to recombination, notably in the presence of strand breaks. These breaks may arise upon genotoxic aggression or when replication forks are stalled to avoid collision between the transcription and replication machineries (Rothstein et al., 2000). Interestingly, PARP-1 and PARP-2 were shown to interact with factors involved in recombination processes present in the nucleolus, such as DNA-PKcs, Ku or WRN (Higashiura et al., 1992; Kuhn et al., 1995; Marciniak et al., 1998; Ruscetti et al., 1998; von Kobbe et al., 2003). A recent report indicated that PARP-1 is required for the reactivation of stalled replication forks imposed by hydroxyurea (Yang et al., 2004). Interestingly, B23 was found together with PARP-1 and C23 in a multiprotein complex, SWAP, involved in B-cell specific recombination (Borggrefe et al., 1998). B23 was shown to promote single-strand DNA reannealing and the formation of joint molecules in a D-loop assay between particular switch regions of immunoglobulin genes involved in class switch recombination. PARP-1 or PARP-2 could be involved in the recognition of such structures that could arise in repetitive DNA regions. One example of such a structure is the T-loop-D-loop formed at telomeres, which is bound by TRF2, a PARP-2 telomeric partner (Dantzer et al., 2004).

A function of DNA damage-dependent PARPs in the surveillance of repetitive DNA was previously described for centromeres and telomeres. PARP-2 (and PARP-1) transiently accumulates at kinetochores during mitosis (Saxena et al., 2002). The genomic instability of centromeric regions observed in bone marrow cells of irradiated PARP-$2^{-/-}$ mice suggests that PARP-2 is required for the correct segregation of chromosomes during mitosis (Menissier de Murcia et al., 2003). In addition, PARP-2, through its functional interaction with the telomeric protein TRF2, is also probably a guardian of the telomeres that have to be prevented from being recognized as double strand breaks. The absence of PARP-2 in murine fibroblasts leads to an alteration of telomere integrity, with some chromosome ends lacking telomeres and an increased heterogeneity of telomere length (Dantzer et al., 2004). Therefore, DNA damage-dependent PARPs play a role in the surveillance of repeated DNA sequences, accounting for the presence of these guardians of the genome in the nucleolus.

We thank F. Dantzer, J. Ménissier-de Murcia and O. Becherel for helpful discussions, J. C. Amé and J. L. Vonesch for advice on microscope analyses and P. Robinson for critical reading of the manuscript. We are grateful to I. Grummt for providing plasmids and antibodies, and P. K. Chan for the anti-B23 antibody. This work was supported by Association pour la Recherche Contre le Cancer, Comité du Haut-Rhin de la Ligue Contre le Cancer, Electricité de France, Commissariat à l'Energie Atomique, Centre National de la Recherche Scientifique and Altana Pharma (Konstanz, Germany).

References

Al-Baker, E. A., Boyle, J., Harry, R. and Kill, I. R. (2004). A p53-independent pathway regulates nucleolar segregation and antigen translocation in response to DNA damage induced by UV irradiation. *Exp. Cell Res.* **292**, 179-186.

Alvarez-Gonzalez, R., Spring, H., Muller, M. and Burkle, A. (1999). Selective loss of poly(ADP-ribose) and the 85-kDa fragment of poly(ADP-ribose) polymerase in nucleoli during alkylation-induced apoptosis of HeLa cells. *J. Biol. Chem.* **274**, 32122-32126.

Amé, J. C., Rolli, V., Schreiber, V., Niedergang, C., Apiou, F., Decker, P., Muller, S., Hoger, T., Menissier-de Murcia, J. and de Murcia, G. (1999). PARP-2, A novel mammalian DNA damage-dependent poly(ADP-ribose) polymerase. *J. Biol. Chem.* **274**, 17860-17868.

Amé, J. C., Spenlehauer, C. and de Murcia, G. (2004). The PARP superfamily. *Bioessays* **26**, 1-12.

Andersen, J. S., Lyon, C. E., Fox, A. H., Leung, A. K., Lam, Y. W., Steen, H., Mann, M. and Lamond, A. I. (2002). Directed proteomic analysis of the human nucleolus. *Curr. Biol.* **12**, 1-11.

Borggrefe, T., Wabl, M., Akhmedov, A. T. and Jessberger, R. (1998). A B-cell-specific DNA recombination complex. *J. Biol. Chem.* **273**, 17025-17035.

Bradsher, J., Auriol, J., Proietti de Santis, L., Iben, S., Vonesch, J. L., Grummt, I. and Egly, J. M. (2002). CSB is a component of RNA pol I transcription. *Mol. Cell* **10**, 819-829.

Chatton, B., Bahr, A., Acker, J. and Kedinger, C. (1995). Eukaryotic GST fusion vector for the study of protein-protein associations in vivo: application to interaction of ATFa with Jun and Fos. *Biotechniques* **18**, 142-145.

Chomczynski, P. and Sacchi, N. (1987). Single-step method of RNA isolation by acid guanidinium thiocyanate-phenol-chloroform extraction. *Anal. Biochem.* **162**, 156-159.

Ciarmatori, S., Scott, P. H., Sutcliffe, J. E., McLees, A., Alzuherri, H. M., Dannenberg, J. H., te Riele, H., Grummt, I., Voit, R. and White, R. J. (2001). Overlapping functions of the pRb family in the regulation of rRNA synthesis. *Mol. Cell. Biol.* **21**, 5806-5814.

Colombo, E., Marine, J. C., Danovi, D., Falini, B. and Pelicci, P. G. (2002). Nucleophosmin regulates the stability and transcriptional activity of p53. *Nat. Cell Biol.* **4**, 529-533.

Dantzer, F., Giraud-Panis, M. J., Jaco, I., Ame, J. C., Schultz, I., Blasco, M., Koering, C. E., Gilson, E., Menissier-de Murcia, J., de Murcia, G. et al. (2004). Functional interaction between poly(ADP-Ribose) polymerase 2 (PARP-2) and TRF2: PARP activity negatively regulates TRF2. *Mol. Cell. Biol.* **24**, 1595-1607.

Desnoyers, S., Kaufmann, S. H. and Poirier, G. G. (1996). Alteration of the

nucleolar localization of poly(ADP-ribose) polymerase upon treatment with transcription inhibitors. *Exp. Cell Res.* **227**, 146-153.

Dundr, M. and Misteli, T. (2001). Functional architecture in the cell nucleus. *Biochem. J.* **356**, 297-310.

Fakan, S., Leduc, Y., Lamarre, D., Brunet, G. and Poirier, G. G. (1988). Immunoelectron microscopical distribution of poly(ADP-ribose)polymerase in the mammalian cell nucleus. *Exp. Cell Res.* **179**, 517-526.

Feuerstein, N., Chan, P. K. and Mond, J. J. (1988). Identification of numatrin, the nuclear matrix protein associated with induction of mitogenesis, as the nucleolar protein B23. Implication for the role of the nucleolus in early transduction of mitogenic signals. *J. Biol. Chem.* **263**, 10608-10612.

Gray, M. D., Wang, L., Youssoufian, H., Martin, G. M. and Oshima, J. (1998). Werner helicase is localized to transcriptionally active nucleoli of cycling cells. *Exp. Cell Res.* **242**, 487-494.

Higashiura, M., Shimizu, Y., Tanimoto, M., Morita, T. and Yagura, T. (1992). Immunolocalization of Ku-proteins (p80/p70): localization of p70 to nucleoli and periphery of both interphase nuclei and metaphase chromosomes. *Exp. Cell Res.* **201**, 444-451.

Kalderon, D., Richardson, W. D., Markham, A. F. and Smith, A. E. (1984). Sequence requirements for nuclear location of simian virus 40 large-T antigen. *Nature* **311**, 33-38.

Kaufmann, S. H., Desnoyers, S., Ottaviano, Y., Davidson, N. E. and Poirier, G. G. (1993). Specific proteolytic cleavage of poly(ADP-ribose) polymerase: an early marker of chemotherapy-induced apoptosis. *Cancer Res.* **53**, 3976-3985.

Kraus, W. L. and Lis, J. T. (2003). PARP goes transcription. *Cell* **113**, 677-683.

Kuhn, A., Gottlieb, T. M., Jackson, S. P. and Grummt, I. (1995). DNA-dependent protein kinase: a potent inhibitor of transcription by RNA polymerase I. *Genes Dev.* **9**, 193-203.

Kurl, R. N. and Jacob, S. T. (1985). Characterization of a factor that can prevent random transcription of cloned rDNA and its probable relationship to poly(ADP-ribose) polymerase. *Nucleic Acids Res.* **13**, 89-101.

Leitinger, N. and Wesierska-Gadek, J. (1993). ADP-ribosylation of nucleolar proteins in HeLa tumor cells. *J. Cell Biochem.* **52**, 153-158.

Liu, W. H. and Yung, B. Y. (1998). Mortalization of human promyelocytic leukemia HL-60 cells to be more susceptible to sodium butyrate-induced apoptosis and inhibition of telomerase activity by down-regulation of nucleophosmin/B23. *Oncogene* **17**, 3055-3064.

Marciniak, R. A., Lombard, D. B., Johnson, F. B. and Guarente, L. (1998). Nucleolar localization of the Werner syndrome protein in human cells. *Proc. Natl. Acad. Sci. USA* **95**, 6887-6892.

Masson, C., Andre, C., Arnoult, J., Geraud, G. and Hernandez-Verdun, D. (1990). A 116,000 Mr nucleolar antigen specific for the dense fibrillar component of the nucleoli. *J. Cell Sci.* **95**, 371-381.

Ménissier de Murcia, J., Niedergang, C., Trucco, C., Ricoul, M., Dutrillaux, B., Mark, M., Olivier, F. J., Masson, M., Dierich, A., LeMeur, M. et al. (1997). Requirement of poly(ADP-ribose)polymerase in recovery from DNA damage in mice and in cells. *Proc. Natl. Acad. Sci. USA* **94**, 7303-7307.

Menissier de Murcia, J., Ricoul, M., Tartier, L., Niedergang, C., Huber, A., Dantzer, F., Schreiber, V., Ame, J. C., Dierich, A., LeMeur, M. et al. (2003). Functional interaction between PARP-1 and PARP-2 in chromosome stability and embryonic development in mouse. *EMBO J.* **22**, 2255-2263.

Mosgoeller, W., Steiner, M., Hozak, P., Penner, E. and Wesierska-Gadek, J. (1996). Nuclear architecture and ultrastructural distribution of poly(ADP-ribosyl)transferase, a multifunctional enzyme. *J. Cell Sci.* **109**, 409-418.

Okano, S., Lan, L., Caldecott, K. W., Mori, T. and Yasui, A. (2003). Spatial and temporal cellular responses to single-strand breaks in human cells. *Mol. Cell. Biol.* **23**, 3974-3981.

Panse, S. L., Masson, C., Heliot, L., Chassery, J. M., Junera, H. R. and Hernandez-Verdun, D. (1999). 3-D organization of ribosomal transcription units after DRB inhibition of RNA polymerase II transcription. *J. Cell Sci.* **112**, 2145-2154.

Perry, R. P. and Kelley, D. E. (1970). Inhibition of RNA synthesis by actinomycin D: characteristic dose-response of different RNA species. *J. Cell Physiol.* **76**, 127-139.

Ramsamooj, P., Notario, V. and Dritschilo, A. (1995). Modification of nucleolar protein B23 after exposure to ionizing radiation. *Radiat. Res.* **143**, 158-164.

Rothstein, R., Michel, B. and Gangloff, S. (2000). Replication fork pausing and recombination or "gimme a break". *Genes Dev.* **14**, 1-10.

Rouleau, M., Aubin, R. A. and Poirier, G. G. (2004). Poly(ADP-ribosyl)ated chromatin domains: access granted. *J. Cell Sci.* **117**, 815-825.

Roussel, P., Andre, C., Masson, C., Geraud, G. and Hernandez-Verdun, D. (1993). Localization of the RNA polymerase I transcription factor hUBF during the cell cycle. *J. Cell Sci.* **104**, 327-337.

Rubbi, C. P. and Milner, J. (2003). Disruption of the nucleolus mediates stabilization of p53 in response to DNA damage and other stresses. *EMBO J.* **22**, 6068-6077.

Ruscetti, T., Lehnert, B. E., Halbrook, J., le Trong, H., Hoekstra, M. F., Chen, D. J. and Peterson, S. R. (1998). Stimulation of the DNA-dependent protein kinase by poly(ADP-ribose) polymerase. *J. Biol. Chem.* **273**, 14461-14467.

Savkur, R. S. and Olson, M. O. (1998). Preferential cleavage in pre-ribosomal RNA byprotein B23 endoribonuclease. *Nucleic Acids Res.* **26**, 4508-4515.

Saxena, A., Wong, L. H., Kalitsis, P., Earle, E., Shaffer, L. G. and Choo, K. H. (2002). Poly(ADP-ribose) polymerase 2 localizes to mammalian active centromeres and interacts with PARP-1, Cenpa, Cenpb and Bub3, but not Cenpc. *Hum. Mol. Genet.* **11**, 2319-2329.

Scherl, A., Coute, Y., Deon, C., Calle, A., Kindbeiter, K., Sanchez, J. C., Greco, A., Hochstrasser, D. and Diaz, J. J. (2002). Functional proteomic analysis of human nucleolus. *Mol. Biol. Cell* **13**, 4100-4109.

Schreiber, V., Molinete, M., Boeuf, H., de Murcia, G. and Menissier-de Murcia, J. (1992). The human poly(ADP-ribose) polymerase nuclear localization signal is a bipartite element functionally separate from DNA binding and catalytic activity. *EMBO J.* **11**, 3263-3269.

Schreiber, V., Ame, J. C., Dolle, P., Schultz, I., Rinaldi, B., Fraulob, V., Menissier-de Murcia, J. and de Murcia, G. (2002). Poly(ADP-ribose) polymerase-2 (PARP-2) is required for efficient base excision DNA repair in association with PARP-1 and XRCC1. *J. Biol. Chem.* **277**, 23028-23036.

Schreiber, V., Ricoul, M., Amé, J. C., Dantzer, F., Meder, V. S., Spenlehauer, C., Stiegler, P., Niedergang, C., Sabatier, L., Favaudon, V. et al. (2005). PARP-2, structure-function relationship. In *Poly(ADP-Ribosyl)ation* (ed. A. Bürkle): Landes Bioscience (in press).

Shiratori, M., Suzuki, T., Itoh, C., Goto, M., Furuichi, Y. and Matsumoto, T. (2002). WRN helicase accelerates the transcription of ribosomal RNA as a component of an RNA polymerase I-associated complex. *Oncogene* **21**, 2447-2454.

Slattery, E., Dignam, J. D., Matsui, T. and Roeder, R. G. (1983). Purification and analysis of a factor which suppresses nick-induced transcription by RNA polymerase II and its identity with poly(ADP-ribose) polymerase. *J. Biol. Chem.* **258**, 5955-5959.

Spector, D. L., Ochs, R. L. and Busch, H. (1984). Silver staining, immunofluorescence, and immunoelectron microscopic localization of nucleolar phosphoproteins B23 and C23. *Chromosoma* **90**, 139-148.

Stevnsner, T., May, A., Petersen, L. N., Larminat, F., Pirsel, M. and Bohr, V. A. (1993). Repair of ribosomal RNA genes in hamster cells after UV irradiation, or treatment with cisplatin or alkylating agents. *Carcinogenesis* **14**, 1591-1596.

Szebeni, A. and Olson, M. O. (1999). Nucleolar protein B23 has molecular chaperone activities. *Protein Sci.* **8**, 905-912.

Trucco, C., Oliver, F. J., de Murcia, G. and Menissier-de Murcia, J. (1998). DNA repair defect in poly(ADP-ribose) polymerase-deficient cell lines. *Nucleic Acids Res.* **26**, 2644-2649.

Tulin, A., Stewart, D. and Spradling, A. C. (2002). The Drosophila heterochromatic gene encoding poly(ADP-ribose) polymerase (PARP) is required to modulate chromatin structure during development. *Genes Dev.* **16**, 2108-2119.

von Kobbe, C., Harrigan, J. A., May, A., Opresko, P. L., Dawut, L., Cheng, W. H. and Bohr, V. A. (2003). Central role for the Werner syndrome protein/poly(ADP-ribose) polymerase 1 complex in the poly(ADP-ribosyl)ation pathway after DNA damage. *Mol. Cell. Biol.* **23**, 8601-8613.

Yang, Y. G., Cortes, U., Patnaik, S., Jasin, M. and Wang, Z. Q. (2004). Ablation of PARP-1 does not interfere with the repair of DNA double-strand breaks, but compromises the reactivation of stalled replication forks. *Oncogene* **23**, 3872-3882.

Yu, Y. N., Ding, C., Cai, Z. N. and Chen, X. R. (1986). Cell cycle effects on the basal and DNA-damaging-agent-stimulated ADPRT activity in cultured mammalian cells. *Mutat. Res.* **174**, 233-239.